MONTE CARLO SIMULATION OF MESOSCOPIC PHASE STRUCTURES IN THE NEAR-CRITICAL FLUID USING A "SLENDER STICK" CELL

Yoshio Morioka[1], Masaharu Komiyama[1,2*]

[1]Clean Energy Research Centre, University of Yamanashi, Japan
[2]HICoE–Centre for Biofuel and Biochemical Research, Department of Chemical Engineering, Universiti Teknologi PETRONAS, Malaysia

Received: 14 October 2022 , Accepted: 17 January 2023, Published: 28 April 2023, Publisher: UTP Press, Creative Commons: CC BY 4.0

ABSTRACT

A novel "slender stick" cell was designed to accomplish the unachievable visualisation of fluids' mesoscopic phase behaviour in its near-critical state by using Monte Carlo simulations within the grand canonical ensemble. The simulation clearly showed the two-phase nature, viz., droplets and voids, of Xe just above its critical point ($T_r = T/T_c = 1.01$ and $P_r = P/P_c = 1.09$). The average sizes of supercritical Xe local structures were determined from the cluster size distributions, which agreed well with the published hydrodynamic radii of clusters obtained experimentally through optical methods. The cluster diameter monotonously increased with the fluid density at a constant temperature ($T_r = T/T_c = 1.01$).

Keywords: *Monte Carlo simulation, Mesoscopic structure, Xe, Near-critical state, cluster radii*

INTRODUCTION

The existence of criticality in a gas-liquid phase diagram has fascinated students in chemistry classes, researchers in theoretical and experimental laboratories and engineers in various industries ever since its theoretical formulation by van der Waals [1]. Supercritical fluids have been applied to various industrial processes such as food flavour extraction, epoxide hydration, and nano-particle synthesis. Its recent applications include biomass gasification and liquefaction using supercritical water and other solvents [2]-[3]. Despite their widespread use, however, understanding the nature of supercritical fluids is still a topic of contemporaries. Local density fluctuation due to clusters or mesophase is found to be one of the fundamental factors determining the physicochemical properties of supercritical fluids [4]. Experimental studies involving light scattering [5], small-angle X-ray scattering [6], or neutron scattering [7] have been performed to probe the local structure of supercritical fluids and determine their density fluctuations and cluster hydrodynamic radii. On the other hand, thermodynamic investigations led to a finding that beyond the critical point and in direct continuation from the gas-liquid coexistence line, there exist divides, known as Widom lines, which are loci of maxima to many thermodynamic quantities such as the isobaric heat capacity, the isothermal compressibility and the thermal expansion coefficient [8]. Based on the Gibbs phase rule, Woodcock [9] discusses that the critical state forms a line in a ρ-P diagram, and the "critical point" in the P-T plane is, in effect, a "double point" from where two percolation transition lines extending toward higher T and P region. He notes that over these two lines, isothermal compressibility, heat capacity and thermal expansivity all undergo some degree of change, most likely maxima or minima.

Apparently, the local structure investigations of fluids beyond their critical states are still the frontier. It is noted that experimental data on the structures of supercritical mesophase probed by the above-mentioned experimental methods are average pictures and not the structures of individual mesoscopic phases fluctuating locally. One method to make such varying structures visible is molecular simulation. However, simulations near and/or beyond the critical state—a range dominated by mesoscopic phase fluctuations—are limited, primarily because it is necessary to employ a large unit cell that contains a prohibitively large number of molecules for the calculation to be meaningful. Several methods, such as the use of the Gibbs ensemble [10] and the Ising model [11], have been proposed to circumvent this problem. While these techniques were considered successful, the employed cell sizes were still not large enough to visualise the coexistence of multiple mesoscopic clusters.

METHODS

In this study, we approached the problem by introducing a novel "slender stick" simulation cell that allowed enough space for the coexistence of mesophases near the critical region. The schematics of the proposed simulation cell are shown in Figure 1. It consists of a rectangular parallelepiped with a square base of width W and a very large aspect ratio L/W. The longitudinal length L was determined and fixed at the beginning of the simulation according to parameters such as temperature, pressure, and the number of molecules. Using such a cell enabled simulations in the submicron dimensions along the longitudinal axis with small molecules (<10000). A periodic boundary condition was applied to all six surfaces of the parallelepiped.

*Corresponding author.
E-mail address : masaharu.komiyama@utp.edu.my; masaharu@yamanashi.ac.jp; komiyama@cornell.edu

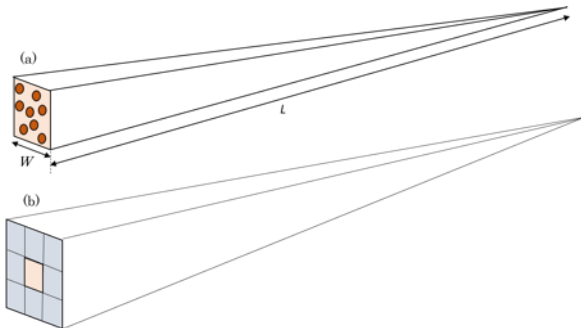

Figure 1 Schematic representation of the proposed "slender stick" simulation cell. (a) Single-cell rectangular parallelepiped with a very large aspect ratio L/W. A periodic boundary condition was applied to all six surfaces of the parallelepiped. (b) The parallelepiped shown in (a) is surrounded by eight of its replicas; molecular contributions from these eight parallelepipeds are considered when calculating the central cell potential

Contributions from the molecules of neighbouring eight parallelepipeds that share longitudinal ridges are considered when calculating the potential of the molecules within the central cell. This is essential to limit the range of the used potential (here, we employed Lennard-Jones, L-J) to 1.5 W on average. It is known that when coexisting vapour-liquid phases are present, the simulation results are very sensitive to potential cut-off ranges in Gibbs ensemble Monte Carlo simulation with ab initio potentials [12]. A similar instability was also observed in the present simulation when W was less than 4.78σ with σ being the L-J distance parameter.

Grand canonical Monte Carlo (MC) simulations were performed using the 6-12 L-J potential:

$$u(r) = 4\varepsilon\{(\sigma/r)^{12} - (\sigma/r)^{6}\} \quad (1)$$

Xenon was chosen as the first test fluid. In order to simulate the actual thermodynamic properties of the fluid, the L-J parameters σ and ε were obtained by a trial and error method that accurately reproduces the Xe P-V diagram near its critical state (T_c = 289.7 K and P_c = 5.84 MPa); σ and ε were determined to be 0.3278 nm and 0.328 x 10^{-20} J, respectively. Furthermore, the condition that the isotherm at the critical state must be horizontal (dP/dV = 0) was also imposed in the trial and error. The chemical potential μ was derived from the system pressure P with the ideal gas approximation using the relation:

$$\mu = kT\, ln(\lambda^3 P / kT) \quad (2)$$

where λ is the thermal de Broglie wavelength; k, Boltzmann constant; and T, absolute temperature.

Most simulations were started with a few thousand molecules. For a set of temperatures and pressure, at least 100 000 MC calculation cycles were performed, and the fluctuations in the molar volume of the system during these cycles were recorded (Figure 2). After a set number of calculation cycles, the entire iteration data were averaged to give a single data set for the given temperature and pressure.

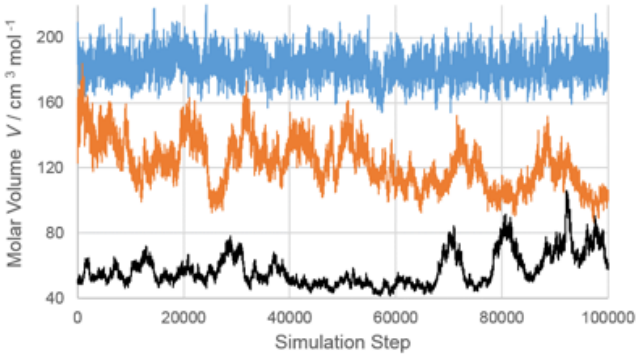

Figure 2 Time courses of three representative simulations performed at pressures of 5.95 MPa (top, $P_r = P/P_c$ = 1.02), 6.13 MPa (middle, P_r = 1.05), and 6.20 MPa (bottom, P_r = 1.06) and at a temperature of 293 K ($T_r = T/T_c$ = 1.01), shown as a function of molar volume that is averaged over the entire cell

RESULTS AND DISCUSSION

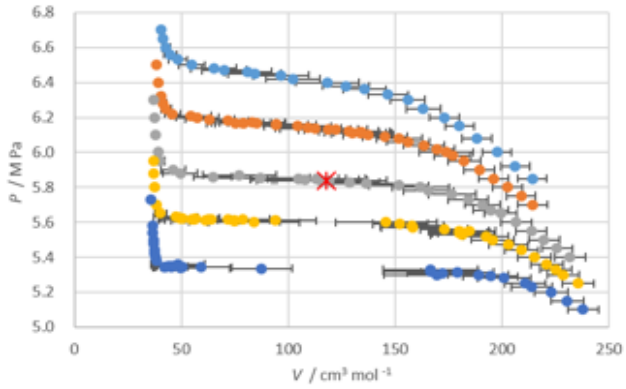

Figure 3 P-V diagram constructed from the simulations with various temperatures and pressures. Error bars show the standard deviations of the molar volume (V) fluctuations within each 100000-iteration set, shown in Figure 2. The critical point is represented by an asterisk. Simulation temperatures are (from top to bottom): 296.0 K, 293.0 K, 289.7 K, 287.0 K, and 284.0 K

Figure 3 shows a P-V diagram constructed from the simulations performed within a temperature range of 284.0–296.0 K and a pressure range of 5.1–6.7 MPa. Each data point is accompanied by an error bar to show the standard deviation of the molar volume fluctuations, found in Figure 2, within each 100000-iteration set. An asterisk represents the critical point in the figure. It is noteworthy that, in the present simulation, the P-V isotherms at and immediately above the critical temperature (289.7 K) are well simulated. Furthermore, the two-phase coexistence region below the critical temperatures was also reproduced stably in our simulations. To the best of our knowledge, this is the first demonstration of a molecular simulation that can seamlessly transition into the two-phase coexisting region from the outer single-phase regions.

Figure 4 shows the snapshot of the 36869th iteration of a simulation at a temperature of 293.0 K ($T_r = T/T_c$ = 1.01) and a pressure of 6.35 MPa ($P_r = P/P_c$ = 1.09), viewed from one long side of the "slender stick" cell shown in Figure 1a. The small circles represent individual Xe atoms.

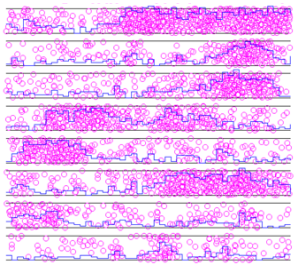

Figure 4 Snapshot of the 36869th iteration of a simulation with T = 293.0 K (T_r = 1.01) and P = 6.35 MPa (P_r = 1.09), viewing Xe molecules (small circles) from one long side of the "slender stick" cell (Figure 1a). The longitudinal axis of the cell is broken into 8 columns in order to fit the entire cell within the figure. The left end of the bottommost column corresponds to the closest end of the "slender stick" cell shown in Figure 1a), and the right end of the topmost column corresponds to the other end of the cell; all the other columns in Figure 4 are connected end-to-end to each other

The longitudinal axis of the cell is broken into 8 columns in order to fit the entire cell within the figure. The number of molecules at this point of the simulation was 3546 (with an initial number of 3000), and the average molar volume was 93.06 cm^3 mol^{-1}.

This figure clearly shows that the system consists of two phases, namely droplets and voids, and these phases can be easily distinguished by the density differences. It is also apparent that the lengths (and hence the volumes) of the low-density (voids) and high-density (droplets) phases vary from place to place in the "slender stick" unit cell, indicating the fractal nature of these droplets and bubbles near the critical state.

Taking advantage of the molecular simulations that can count the atoms in the individual clusters or mesophases, we attempted to determine the size distribution of the high-density mesophase clusters. As exemplified in Figure 5, Cluster size distributions were obtained by counting the filled volume fraction at each cross-section along the longitudinal axis (Figure 4) using a frequency histogram and classifying regions with a filled volume fraction above 0.5 as formed clusters. Figure 5, obtained along the isotherm at 293.0 K (T_r = 1.01), shows that the cluster diameter distribution

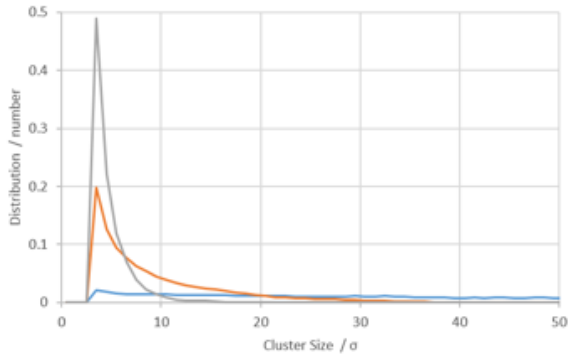

Figure 5 Cluster diameter distributions along the isotherm at 293.0 K (the second isotherm from the top is shown in Figure 3). Densities of the data shown in this figure are 0.0053 mol cm^{-3} (the sharpest distribution, ρ_r = 0.63), 0.0086 mol cm^{-3} (middle distribution, ρ_r = 1.02), and 0.0260 mol cm^{-3} (the broadest distribution, ρ_r = 3.07)

widens as it moves from a low average density (low pressure) to higher average densities (higher pressures).

From the cluster size distributions shown in Figure 5, the mean cluster diameter was calculated for each set of T and ρ. Figure 6 shows the density dependence of mean cluster diameter for 293.0 K (the second isotherm from the top in Figure 3).

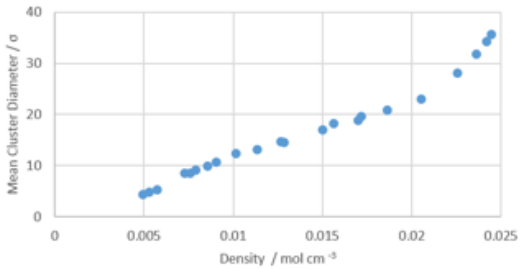

Figure 6 Variation in mean cluster diameter along the second isotherm from the top (293.0 K) in Figure 3, as a function of molar density

The obtained simulation data was compared with the average cluster sizes that were experimentally obtained using optical scattering. Table 1 lists the present simulation data at a reduced density ρ_r of 1.00, which was non-dimensionalised by dividing it by 2σ, along with similarly non-dimensionalised Xe cluster radii measured and reported [13].

Table 1 Comparison of the non-dimensionalised Xe cluster radii at a reduced density ρ_r of 1.00 obtained by the present simulation and by optical scattering [13]

T_r	Non-dimensionalised Xe cluster radii	
	Present simulation	Hydrodynamic radii from optical scattering*
1.01	5.0	7.5
1.02	4.1	4.0

*Data were taken from Figure 3 of reference [13]

The similarity between the simulation and experimental values is striking, considering the fact that the present simulation employs simplistic L-J potential and that the cluster size is measured only on one dimension. This suggests that the observed similarity between the two methods compared in Table 1 is more of a coincidence than a necessity. Nevertheless, this similarity indicates that the proposed simulation technique is an effective means to probe the local structures of the supercritical fluid.

CONCLUSION

Employing the novel "slender stick" cell in a Monte Carlo simulation within a grand canonical ensemble enabled us to probe fluid structures in the proximity of its critical state. The simulation could quantitatively replicate the P-V diagram in the critical region, heretofore not possible. Biphasic structures just above the critical state were visualised, and the mesoscopic fluctuations were characterised using cluster size distributions. The effectiveness of

the proposed simulation methodology was proven by the close correspondence of our results with available experimental data on the average cluster size of Xe in the supercritical state. The proposed methodology would provide a useful platform for probing the local structure and thermodynamic characteristics of near-critical and supercritical fluid, including their behaviours across Widom lines [8] and their characteristics as reaction media.

ACKNOWLEDGEMENTS

Support from the Ministry of Education Malaysia through HICoE award to the Centre for Biofuel and Biochemical Research is duly acknowledged.

REFERENCES

[1] J.D. van der Waals, Over de Continuïteit van den Gasen Vloeistoftoestand, Ph.D. Thesis, Leiden, The Netherlands 1873.

[2] L. Tiong, and M. Komiyama, "Statistical analysis of microalgae supercritical water gasification: Reaction variables, catalysis and reaction pathways", *Journal of Supercritical Fluids,* vol. 183, p. 105552, 2022, doi: 10.1016/j.supflu.2018.05.011.

[3] F.Y. Han, M. Komiyama, Y. Uemura, and N.E. Rabat, "Catalytic alcohothermal liquefaction of wet microalgae with supercritical methanol", *Journal of Supercritical Fluids*, vol. 157, p. 104704, 2020, doi: 10.1016/j.supflu.2019.104704.

[4] L.S. Ornstein and F. Zernike, "Accidental deviations of density and opalescence at the critical point of a single substance", *Proceedings Academy of Arts Sciences, vol. 17*, pp. 793–806, 1914.

[5] H.L. Swinney and D.L. Henry, "Dynamics of fluids near the critical point: decay rate of order-parameter fluctuations", *Physical Review A*, vol. 8, pp. 2586–2617, 1973, doi: 10.1103/PhysRevA.8.2586.

[6] K. Nishikawa and I. Tanaka, "Correlation lengths and density fluctuations in supercritical states of carbon dioxide", *Chemical Physics Letters*, vol. 244, pp. 149–152, 1995, doi: 1016/0009-2614(95)00818-O.

[7] T. Yamaguchi, "Structure of subcritical and supercritical hydrogen-bonded liquids and solutions", *Journal of Molecular Liquids*, vol. 78, no. 1-2, pp. 43–50, 1998, doi: 10.1016/S0167-7322(98)00083-X.

[8] V.V. Brazhkin, Yu.D. Fomin, A.G. Lyapin, V.N. Ryzhov, and E.N. Tsiok, "Widom line for the liquid–gas transition in Lennard-Jones system", *Journal of Physical Chemistry B*, vol. 115, pp. 14112–14115, 2011, doi: 10.1021/jp2039898.

[9] L.V. Woodcock, "Observations of a thermodynamic liquid–gas critical coexistence line and supercritical fluid phase bounds from percolation transition loci", *Fluid Phase Equilibria*, vol. 351, pp. 25–33, 2013, doi: 10.1016/j.fluid.2012.08.029.

[10] A.Z. Panagiotopoulos, "Monte Carlo methods for phase equilibria of fluids", *Journal of Physics: Condensed Matter*, vol. 12, no. 3, pp. R25–R52,2000, doi: 10.1088/0953-8984/12/3/201.

[11] N.B. Wilding, "Critical-point and coexistence-curve properties of the Lennard-Jones fluid: a finite-size scaling study", *Physical Review E*, vol. 52, pp. 602–611, 1995, doi: 10.1103/physreve.52.602.

[12] P.S. Vogt, R. Liapine, B. Kirchner, A.J. Dyson, H. Huber, G. Marcelli, and R.J. Sadus, "Molecular simulation of the vapour–liquid phase coexistence of neon and argon using ab initio potentials", *Physical Chemistry Chemical Physics, vol. 3*, pp. 1297–1302, 2001, doi: 10.1039/B008061F.

[13] D. Kajiya, K. Nishikawa, and K. Saitow, "Time Evolution of Density Fluctuation in the Supercritical Region. 2. Comparison of Hydrogen- and Non-hydrogen-Bonded Fluids", *Journal of Physical Chemistry A*, vol. 109, pp. 7365–7370, 2005, doi: 10.1021/jp0522056.